Pharmacokinetics of Methotrexate in the Extracellular Fluid of Brain C6-Glioma After Intravenous Infusion in Rats

Sylvain Dukic,[1,4] Tony Heurtaux,[1] Matthieu L. Kaltenbach,[1] Guillaume Hoizey,[1] Aude Lallemand,[2] Bertrand Gourdier,[3] and Richard Vistelle[1]

Received March 3, 1999; accepted May 6, 1999

Purpose. Establishment of the pharmacokinetic profile of methotrexate (MTX) in the extracellular fluid (ECF) of a brain C6-glioma in rats.
Methods. Serial collection of plasma samples and ECF dialysates after i.v. infusion of MTX (50 or 100 mg/kg) for 4 h. HPLC assay.
Results. Histological studies revealed the presence of inflammation, edema, necrosis, and hemorrhage in most animals. *In vivo* recovery (reverse dialysis) was 10.8 ± 5.3%. MTX concentrations in tumor ECF represented about 1–2% of the plasma concentrations. Rapid equilibration between MTX levels in brain tumor ECF and plasma. ECF concentrations almost reached steady-state by the end of the infusion (4 h), then decayed in parallel with those in plasma. Doubling of the dose did not modify MTX pharmacokinetic parameters ($t_{1/2}\alpha$, $t_{1/2}\beta$, MRT, f_b, Vd, and CL_T), except for a 1.7-fold increase of AUC_{Plasma} and a 3.8-fold increase in AUC_{ECF}, which resulted in a 2.3-fold increase in penetration (AUC_{ECF}/AUC_{Plasma}). In spite of an important interindividual variability, a relationship between MTX concentrations in plasma and tumor ECF could be established from mean pharmacokinetic parameters.
Conclusions. High plasma concentrations promote the penetration of MTX into brain tissue. However, free MTX concentrations in tumor ECF remain difficult to predict consistently.

KEY WORDS: C6-glioma; methotrexate; microdialysis; pharmacokinetics.

INTRODUCTION

To date, most of available data on the distribution of anticancer agents in central nervous system (CNS) has been based on analysis of cerebrospinal fluid (CSF) or tissue homogenates (1–5). These approaches, however, are limited since drug concentrations in CSF or whole tissue do not necessarily reflect those in brain or tumor tissue. In contrast, unbound drug concentrations in extracellular fluid (ECF) provide important information on tissue exposure to the drug, and are often an important determinant of the pharmacological effect. As such, ECF can be viewed as a liquid compartment in the immediate vicinity of cells in which drugs must enter. Since the exposure of tumor cells to free drug in ECF can be considered comparable to that observed *in vitro* in cell cultures, monitoring drug concentrations in ECF may be crucial in understanding the time course of drug effects and to optimize drug dosage regimens.

To our knowledge, only two studies using microdialysis in tumor-bearing rats have been published. One study investigated the effect of a R-6 rhabdomyosarcoma on the penetration of MTX in brain by using transverse dialysis (6). The second study determined ECF MTX concentrations in a RG-2 tumor model (7). Their experimental protocols, however, did not allow reproducible probe positioning within the tumor, which could lead to inaccurate determinations of ECF MTX concentrations from a region surrounding the brain tumor. There is thus a lack of data, obtained under precisely controlled experimental conditions, on the time course of MTX concentrations in brain tumor. Therefore, the purpose of this study was to establish the pharmacokinetic profile of MTX in plasma and ECF following i.v. infusion of MTX (50 or 100 mg/kg) in tumor-bearing rats.

MATERIALS AND METHODS

Drugs and Chemicals

Methotrexate was obtained from Lederlé (Oullins, France). Purified water was obtained from an Alpha-Q purification system (Millipore, Saint-Quentin en Yvelines, France). Cell culture products were obtained from Biomedia (Boussens, France), and all other chemicals were reagent or analytical grade.

Animals

Male Wistar rats weighing 260–300 g (Elevage Dépré, Saint Doulchard, France) were individually housed in a controlled environment (20 ± 2°C; 65 ± 15% relative humidity) and maintained under a 12:12 h light:dark cycle. They were allowed to adapt to the housing environment for at least one week prior to study and had access to food (U.A.R., Villemoisson sur Orge, France) and tap water *ad libitum*. All animal procedures adhered to the "Principles of laboratory animal care" (NIH publication #85-23, revised 1985).

C6 Glioma Cell Line

C6 glioma cells (8) were maintained in Ham F12 minimum essential medium containing 10% fetal calf serum, 0.5% streptomycin, 0.5% penicillin, 0.05% amphotericin B, and 0.5% glutamine. They were grown to confluence in a humidified atmosphere of 5% CO_2 at 37°C, harvested with a solution of 0.05% trypsin and 0.02% EDTA, and resuspended in Ham F12 medium. Cells were washed three times in Ham F12 medium supplemented with 10% fetal calf serum, and counted by a trypan blue dye exclusion method. Finally, they were suspended in Ham F12 minimum essential medium to a final concentration of 5.10^5 cells/µl for intracerebral inoculation.

[1] Laboratoire de Pharmacologie et de Pharmacocinétique, U.F.R. de Pharmacie, Université de Reims Champagne Ardenne, 51096 Reims Cedex, France.
[2] Laboratoire Pol Bouin, Service d'Histologie et de Cytologie, Hôpital Maison-Blanche, CHRU de Reims, Reims, France.
[3] Laboratoire de Pharmacie Clinique, U.F.R. de Pharmacie, Université de Reims Champagne Ardenne, Reims, France.
[4] To whom correspondence should be addressed. (e-mail: sylvain.dukic@univ-reims.fr)

ABBREVIATIONS: AUC_{Plasma}, area under the plasma concentration-time curve from time 0 to the end of the infusion (4 h); AUC_{ECF}, area under the tumor extracellular fluid concentration-time curve from time 0 to the end of the infusion (4 h); BBB, blood-brain barrier; CNS, Central nervous system; ECF, Extracellular fluid; MTX, Methotrexate.

Intracerebral Inoculation of the C6 Glioma Cells

Rats were anesthetized by i.p. injection of xylazine (Bayer, Leverkusen, Germany) 10 mg/kg and ketamine (Parke-Davis, Courbevoie, France) 100 mg/kg. Their head was mounted into a stereotaxic head holder in a flat-skull position, and the skull exposed by a midline incision. A small burr hole was drilled into the right side of the skull at a position 3 mm lateral from midline and 1 mm anterior to the bregma. Four additional holes were drilled for anchor screws several millimeters away from the burr hole. After inserting the anchor screws, a CMA/11 guide cannula (Phymep, Paris, France) was slowly lowered at a depth of 4 mm from the brain surface. The skull was then blotted dry and dental cement (Autenal Dental, Harrow, England) applied to anchor the guide cannula. Ten minutes later, 10 μl of the tumor cell suspension was injected over 2 min by a microsyringe (Exmire, Polylabo, Strasbourg, France) equipped with a needle 1 mm longer than the guide cannula. After a 3 min wait, the needle was removed and the guide cannula capped with a dummy stylet that extended 0.5 mm beyond its tip.

Cerebrovascular Permeability

In order to establish the effect of tumor growth on the permeability of the blood-brain barrier (BBB), cerebrovascular leakage of Evans blue, a marker dye which does not penetrate in the CNS under normal conditions, was evaluated (9). Fourteen days after tumor implantation, 5 rats were anesthetized with isoflurane, and Evans blue injected intravenously (0.5 ml of a 2% solution in saline). One hour later, all blood from the circulation was removed by perfusing the heart with saline (120 ml) and severing the inferior vena cava. The brain was extracted, sliced at the site of implantation of the cannula, and screened for the presence of a blue coloration indicating extravascular leakage of the dye.

Probe Calibration

The efficiency of microdialysis probes was determined by measuring *in vitro* recovery. Probes were placed in vials containing an unstirred Krebs-Ringer solution spiked with MTX (50 μg/ml) and maintained at 38°C. They were perfused with Krebs-Ringer (flow-rate: 7 μl/min) for at least 30 min before collection of 8 dialysates at 15 min intervals. The mean *in vitro* recovery was then computed from all the ratios of MTX concentrations in effluent dialysate to the probed reservoir according to the following equation:

$$\text{Recovery}_{\text{in vitro}} = \frac{C_{\text{dialysate}}}{C_{\text{sample}}}$$

In vivo recovery was estimated by reverse dialysis (10) in a dedicated group of 5 tumor-bearing rats. Upon implantation, microdialysis probes were perfused (flow rate: 7 μl/min) with Krebs-Ringer spiked with MTX (230 ng/ml) for 30 min. Dialysates were then collected every 15 min for 2 hours (n = 8) and the mean *in vivo* recovery computed from all recovery ratios calculated as shown below:

$$\text{Recovery}_{\text{in vivo}} = \frac{C_{\text{in}} - C_{\text{out}}}{C_{\text{in}}} \times 100$$

where C_{in} and C_{out} are the MTX concentrations in the perfusate inflow and outflow, respectively.

Experimental Procedure

Fourteen days after tumor implantation, rats were anesthetized with isoflurane (induction: 5% and maintenance: 1–1.5%) by an Isotec 4 evaporator (Ohmeda, Maurepas, France) and ventilated with a small animal respirator (Harvard Biosciences, Les Ulis, France). They were placed onto a heating pad set at 38°C (Homeothermic Blanket System, Phymep, Paris, France) and end-tidal CO_2 was monitored on a CO_2 analyzer (Engström Eliza, Cambro, Sweden). A catheter (N°3, Biotrol, Paris, France) filled with heparin-saline solution (25000 UI/l, Héparine Choay, Paris, France) was inserted into the right carotid artery and used for blood sampling. Another catheter (N°1, Biotrol) was inserted into the left jugular vein for drug administration.

Microdialysis was carried out with a CMA/100 microinjection pump (Phymep, Paris, France) and CMA/11 probes (membrane length: 2 mm; tip diameter: 240 μm; cutoff: 6 000 Daltons). Probes were perfused with Krebs-Ringer at a flow-rate of 7 μl/min over the duration of the experiment. According to a parallel design, animals were given either 50 mg/kg (n = 6) or 100 mg/kg (n = 6) of MTX as a slow i.v. infusion over 4 h. Dialysates were collected every 15 min for 6 h and blood samples (200 μl) were drawn at the midpoint of dialysis collection periods. They were replaced with an equal amount of heparinized saline and immediately centrifuged. Samples were stored at −20°C until analysis. Methotrexate concentrations were quantified by an isocratic reversed-phase HPLC-UV assay described in details elsewhere (7). Lastly, MTX concentrations in dialysates were corrected by the mean *in vivo* recovery to yield estimations of ECF concentrations.

Histological Studies

Histological studies were performed in order to verify the placement of microdialysis probes within the tumor tissue, and to relate MTX penetration with the sampling site environment. Under deep anesthesia, all blood was removed, and 120 ml of 10% neutral buffered formalin injected to perform in situ fixation. The brains were removed and stored in 4% buffered formaldehyde solution at 4°C. After routine processing (dehydration in a graded alcohol series, paraffin embedding), blocks were serially cut, and every 10^{th} 5 μm section stained with hematoxylin pholine saffron before microscopic examination. The whole path of the semipermeable part of the microdialysis probe and the tumor implantation site were semi-quantitatively examined for severity and extent of edema, necrosis, and inflammation according to an empirical grading system (absent, moderate, or severe). Blood vessel density in and around the tumor tissue (excluding hemorrhagic and necrotic zones) was also estimated by calculating the average number of vessels within five zones under ×40 and ×400 magnification.

Pharmacokinetic and Statistical Analysis

Pharmacokinetic parameters of MTX (V_C, k_{10}, k_{12}, k_{21}, and free fraction in tissue f_{Tu}) were determined for each animal by simultaneous fitting of plasma and tumor ECF concentration-time curves to a two compartment open model by nonlinear least-squares regression (Ph/Edsim Professional 2.05, Mediware, Groningen, The Netherlands). The choice of the model was based on the Akaike information criterion. The area under the concentration-time curve (AUC), the mean residence time

(MRT), the half-life of distribution and elimination ($t_{1/2}\alpha$ and $t_{1/2}\beta$), the systemic clearance (CL_T), and the volume of distribution (Vd_{SS}) were calculated according to standard pharmacokinetic equations (11). The extent of drug transport into tumor ECF (MTX penetration) was computed as the ratio of AUC_{ECF} over AUC_{Plasma} over the duration of MTX infusion (0–4 h). MTX binding to plasma proteins was determined by ultrafiltration on a MPS-1 micropartition system (Amicon, Epernon, France) equipped with a YM-T membrane filter. All results are expressed as mean ± S.D.

In a separate analysis, free MTX concentrations in tumor tissue (C_{Tu}) were predicted from parameters obtained by fitting plasma data alone according to the following equation:

$$C_{Tu} = \frac{f_{Tu}}{V_p} \cdot \left(\frac{k_{12} \cdot K_o}{k_{21} - k_{10}} - \frac{k_{12} \cdot K_o}{\alpha \cdot (\beta - \alpha)} \cdot e^{-\alpha t} - \frac{k_{12} \cdot K_o}{\beta \cdot (\alpha - \beta)} \cdot e^{-\beta t} \right)$$

where f_{Tu} is the average free fraction in tumor tissue (1.25% and 2.55% for the 50 and 100 mg/kg doses, respectively) derived from the individual f_{Tu} values obtained from previous simultaneous fits of plasma and tumor ECF concentration-time curves.

Statistical comparisons of pharmacokinetic parameters were carried out with Statgraphics Plus (Version 1, Manugistics, Rockville, USA). Non-parametric Mann-Whitney U tests (Wilcoxon rank sum test) with the *a priori* level of significance set at $p < 0.05$ were used because the number of animals was small, and there was no certainty that the data were normally distributed.

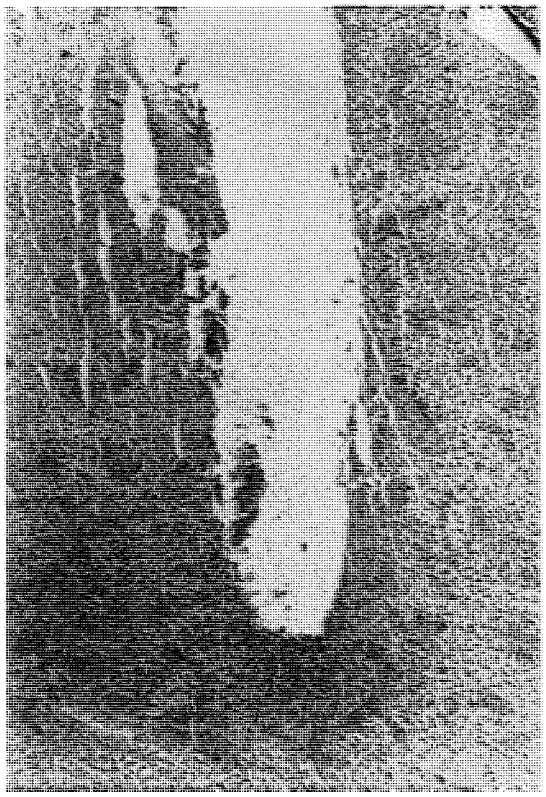

Fig. 1. Photomicrograph of a brain C6 glioma showing the narrow elongated space produced by the passage of the microdialysis probe projecting into the central part of the tumor. The dimension line at the bottom right corner represents 166 μm.

RESULTS

Following tumor implantation, all animals rapidly resumed normal activity without showing ill effects. No loss of appetite, gross behavioral disorders, or neurological signs were observed during the development of the tumor.

Histological Findings

Fourteen days after inoculation, tumor cells formed a mass centered on the injection site with no spread to the contralateral hemisphere. The tumor shape was usually ovoid, with a higher vertical (6.9 ± 1.6 mm) than horizontal diameter (4.2 ± 0.9 mm). Microscopic examinations showed a narrow elongated space produced by the passage of the probe projecting into the central part of the tumor (Fig. 1). They also revealed the presence of moderate to severe inflammation (4 and 6 cases, respectively), edema (4 and 5 cases), necrosis (6 and 4 cases), and hemorrhage (6 and 2 cases) in most animals. The average number of blood vessels in tumor tissue was 2.3 ± 0.5 vs. 3.4 ± 1.1 around the tumor tissue. A significant correlation was found between tumor size and inflammation ($r = -0.6779$) and between tumor size and intra-tumoral vascularization ($r = 0.632$). Similarly, a relationship was observed between AUC_{ECF} and tumor size ($r = -0.6968$), and between AUC_{ECF} and peritumoral vascularization ($r = -0.8633$).

Cerebrovascular Permeability

Evans blue staining was restricted to the tumor tissue (see Fig. 2). Brain tissue adjacent to the tumor and in the contralateral hemisphere was not stained by the dye, thus indicating the BBB may be preserved in those areas.

Plasma Pharmacokinetics

Mean plasma concentration-time profiles of MTX are shown in Fig. 3. Pharmacokinetic parameters are reported in Table I. At the end of infusion, plasma concentrations reached a maximum of 17.3 ± 4.4 μg/ml (range: 10.7–22.3 μg/ml) and 28.5 ± 6.7 μg/ml (range: 19.2–36.5 μg/ml) for the 50 and 100 mg/kg doses, respectively, then declined biexponentially. Taking into account MTX elimination $t_{1/2}$ (ca. 60 min), these maximum concentrations were very close to those one would obtain at steady-state. Half-life, total body clearance, apparent volume of distribution, and protein binding did not differ significantly between the two dose groups, whereas AUC_{Plasma} was proportionally related to the dose (1.7-fold increase).

Tissue Pharmacokinetics

In vitro and *in vivo* recoveries were not significantly different (7.0 ± 0.6% vs. 10.5 ± 6.7%, respectively). Mean concentration-time profiles of MTX in tumor ECF are shown in Fig. 3. Steady state conditions were almost reached by the end of the infusion (4 h) with maximum MTX tumor ECF concentrations of 229 ± 130 ng/ml (range: 63–379 ng/ml) and 772 ± 427 ng/ml (range: 246–1334 ng/ml) for the 50 and 100 mg/kg doses, respectively. After the end of infusion, tumor MTX ECF

Fig. 2. Photography of a brain section showing the distribution of Evans blue used to indicate alterations of cerebrovascular permeability.

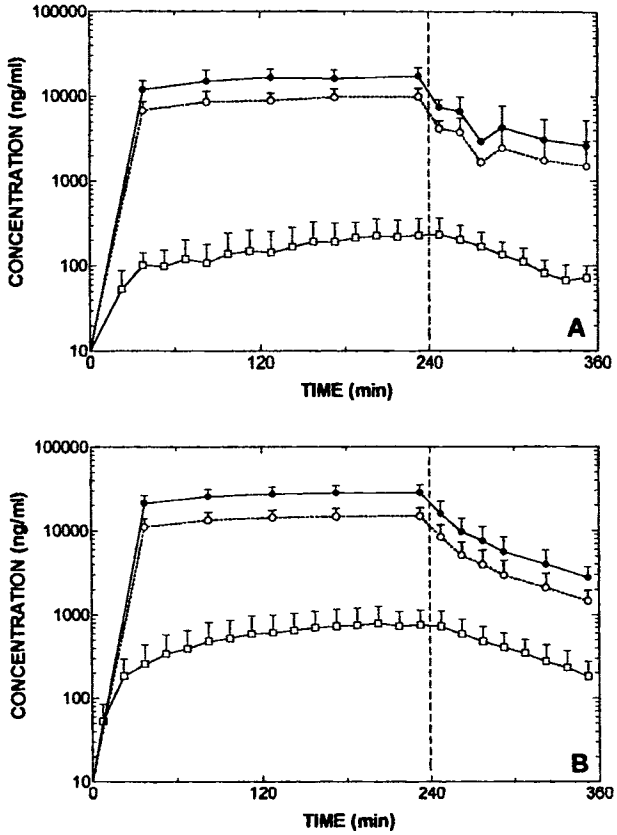

Fig. 3. Plots of total (●) and free (○) methotrexate concentrations in plasma and in tumor extracellular fluid (□) as a function of time in rats following i.v. infusion of 50 (A) or 100 (B) mg/kg (mean ± SD).

concentrations declined in parallel to those observed in plasma. Individual correlation coefficients between ECF and total plasma concentrations are presented in Table II. For both doses, AUC_{ECF} and MTX penetration were subject to marked inter-individual variability. A two-fold increase of the dose resulted in a 3.8-fold increase of the AUC_{ECF}, and in a 2.3-fold increase in MTX penetration.

Pharmacokinetic Simulations

MTX concentration-time profiles in tumor ECF were predicted from pharmacokinetic parameters obtained after fitting plasma data alone. Plots of predicted vs. observed ECF concentrations are shown in Fig. 4. They reveal a huge difference between total concentrations in plasma and free concentrations in tumor tissue. Plasma and ECF concentrations obtained after the 100 mg/kg dose could be reasonably well predicted from the pharmacokinetic parameters of MTX obtained by fitting average concentration-time data of the 50 mg/kg dose (Fig. 5).

DISCUSSION

The C6 brain tumor fulfills commonly accepted criteria for an ideal *in vivo* experimental brain tumor model and has been used in numerous studies (12–15). The procedure used for the implantation of tumor cells (15) and the choice of specific stereotaxic coordinates allowed minimal extracerebral extension of the tumor (16). Moreover, the implantation of a guide cannula offered a unique opportunity to perform both the inoculation of tumor cells and microdialysis in the central part

Table I. Pharmacokinetic Parameters and Penetration Values (AUC_{ECF}/AUC_{Plasma}) of Methotrexate in Brain Tumor-Bearing Rats (n = 6) Following i.v. Infusion of 50 or 100 mg/kg

	50 mg/kg	100 mg/kg
$t_{\frac{1}{2}}\alpha$ (min)	6.8 ± 5.4 (0.3–13.4)	4.6 ± 2.2 (2.1–8.3)
$t_{\frac{1}{2}}\beta$ (min)	78 ± 22 (50–101)	63 ± 20 (42–94)
MRT (min)	159 ± 11 (149–180)	157 ± 4 (153–164)
Vd_{SS} ($l \cdot kg^{-1}$)	0.203 ± 0.089 (0.123–0.350)	0.199 ± 0.052 (0.0133–0.282)
CL_T ($l \cdot h^{-1} \cdot kg^{-1}$)	0.749 ± 0.152 (0.532–1.010)	0.913 ± 0.171 (0.693–1.253)
f_b (%)	43.1 ± 2.9 (39.4–45.9)	47.3 ± 2.4 (44.0–50.0)
AUC_{Plasma} ($\mu g \cdot min \cdot ml^{-1}$)	3315 ± 809 (2338–4574)	5566 ± 1263[a] (6961–3933)
AUC_{ECF} ($\mu \cdot min \cdot ml^{-1}$)	32 ± 21 (11–60)	122 ± 81[a] (37–257)
AUC_{ECF}/AUC_{Plasma} (%)	1.02 ± 0.75 (0.36–2.37)	2.32 ± 1.57[a] (0.54–4.42)

Note: Values are presented as mean ± standard deviation (range).
[a] $p < 0.05$.

Table II. Individual Correlation Coefficients Between Tumor ECF and Plasma Concentrations of MTX After i.v. Infusion of MTX (50 and 100 mg/kg)

	50 mg/kg			100 mg/kg	
Rat N°	During the infusion	After the end of infusion	Rat N°	During the infusion	After the end of infusion
1	0.895	0.926	7	0.943	0.858
2	0.770	0.912	8	0.932	0.749
3	0.734	0.977	9	0.866	0.923
4	0.690	0.891	10	0.864	0.929
5	0.788	0.788	11	0.672	0.975
6	0.630	0.953	12	0.881	0.929

of the tumor, whatever the exact size of the tumor. Commercially available probes with the smallest diameter were used in order to minimize tissue damage. ECF samples were collected by using a high perfusion flow-rate coupled with long sampling times to increase the absolute recovery (i.e., the total amount of drug that is collected within a given time interval). This approach allowed the collection of large enough dialysates as required by the analytical method yet enabled the sampling interval to be compatible with the establishment of a pharmacokinetic profile.

In vivo recovery varied widely between animals, suggesting anatomic differences in the tumor mass since ECF sampling of tumor ECF was always performed at a precise and reproducible location. An alternative approach based on its determination in each animal before performing the pharmacokinetic experiment was however not possible since preliminary MTX administration would have affected tumor growth, intratumoral disposition, and thus the pharmacokinetic parameters of MTX.

The vascular permeability of the C6 tumor was high. This observation, in agreement with data on the cerebrovascular permeability of glioma in rats (17), indicates the tumor itself and/or the experimental procedure used for its implantation may have caused major alterations in the integrity of the BBB. Indeed, vessels in primary gliomas have a discontinuous endothelium (18,19) and intracerebral inoculation rates larger than 1 μl/min may damage the BBB. Lastly, the heterogeneous nature of solid tumors may have contributed to the important inter-individual variability. Brain tissue reactions to the implantation of the probe were also investigated. They revealed the presence of local hemorrhage along the path of the probe. No relationship between the presence and/or the severity of the hemorrhage and MTX penetration could be found. In contrast, a positive correlation between tumor size and intra-tumoral vascularization was noted.

MTX was chosen in this study as a model compound for hydrophilic anticancer drugs. Doses were selected arbitrarily to yield plasma concentrations in the range of those observed in patients receiving high-dose MTX. Plasma concentration-time curves were adequately fitted to a two compartment open-model which provided pharmacokinetic parameters (i.e., Vd and CL_T) similar to those obtained in healthy rats (7,20). These results suggest the presence of a brain C6-glioma did not affect the disposition of MTX at the time of the experiment. The pharmacokinetic parameters of MTX in plasma were not affected by a doubling of the dose, except for an almost two-fold increase of AUC_{Plasma}. These results are in agreement with the linear relationship found between MTX dose (in the 18.75 to 300 mg/kg range) and steady-state MTX concentrations in rats (21). In spite of a known dose-dependent decrease in MTX binding to plasma proteins (22), the value determined in this study remained in the range of that found by Ekstrom et al. in rats (21), and was not significantly different at the two dose levels.

The equilibration between MTX levels in brain tumor ECF and plasma was rapid, confirming the equilibration of drug concentrations between brain and blood is very fast, even for hydrophilic compounds (6,7,23). However, MTX ECF concentrations were much lower than those in plasma, indicating a difference in influx (into the brain tumor) and/or efflux (out of the brain tumor) clearances. Although the exact mechanism underlying this observation remains unknown, contributing factors may include bulk flow (ECF drainage) and the presence of active transport processes into and out of the brain tumor (23) . Moreover, highly ionized at physiological pH (99.8%), MTX does not penetrate the BBB to any great extent under normal conditions. As such, the entry of a hydrophilic drug into brain tumor tissue depends not only on the breakdown of the BBB but also on drug diffusion through the tumor tissue itself (24). The lack of appropriate controls, however, prevented

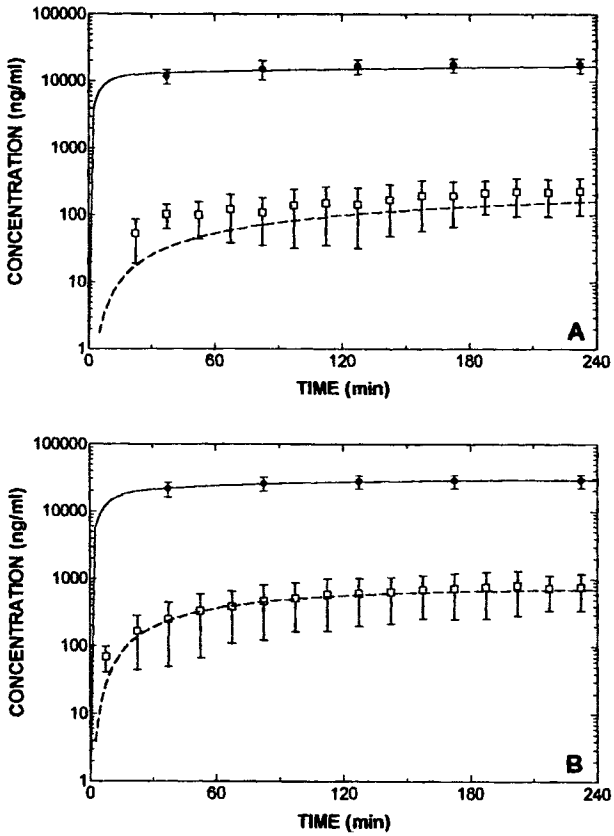

Fig. 4. Computer-fitted (—) versus observed (●) methotrexate concentrations in plasma, and model-predicted (---) versus observed (□) concentrations in tumor extracellular fluid as a function of time following i.v. infusion of 50 (A) or 100 (B) mg/kg in rats (mean ± SD).

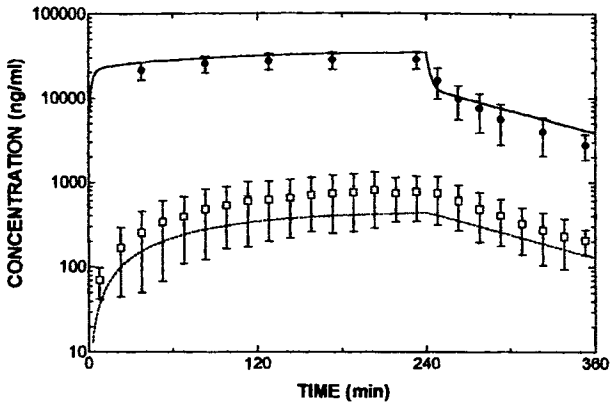

Fig. 5. Computer-predicted versus observed methotrexate concentrations in plasma (●) and in tumor extracellular fluid (□) as a function of time in tumor-bearing rats following i.v. infusion of 100 mg/kg (mean ± SD). Predictions were based on mean pharmacokinetic parameters obtained following i.v. infusion of a 50 mg/kg dose.

us from comparing MTX concentration profiles in tumor ECF to those in normal brain tissue.

Tumor exposure (AUC_{ECF}) was low, yet highly variable, in comparison to AUC_{Plasma} for both doses. Doubling of the dose, however, resulted in an almost four-fold increase of AUC_{ECF} and a two-fold increase of MTX penetration. These findings indicate high plasma concentrations may promote the penetration of MTX into brain tumor tissue, as suggested by experimental and clinical observations (5,25–27).

Mean MTX concentrations in tumor ECF could be predicted with reasonable accuracy from mean pharmacokinetic parameters obtained after fitting plasma data alone. This relationship, however, remains to be validated on a larger scale due to the important inter-individual variability in tumor ECF exposure to MTX. These results also confirm the difficulty in obtaining reliable predictions of free MTX concentrations in brain tumor ECF from individual blood concentration-time curves as evidenced by the important variability of the AUC_{ECF}/AUC_{Plasma} ratios (25–28).

In conclusion, our study demonstrated the uneven distribution and low penetration of MTX into ECF of a brain C6 glioma. Taking into account the rapid equilibrium between plasma and brain tumor ECF, these results suggest an i.v. bolus injection, by inducing an important concentration gradient across the BBB, would be more effective in obtaining high ECF MTX concentrations. Investigations are currently in progress to validate this hypothesis.

ACKNOWLEDGMENTS

Ph/Edsim Professional was kindly provided by Nieko Punt (Mediware B.V., Zernike Park 2, 9747 AN Groningen, The Netherlands). We wish to thank Drs. H. Ferté, and J. Depaquit for technical and photographic assistance. These studies were supported by a grant from ARC (Association por la Recherche contre le Cancer).

REFERENCES

1. E. Chatelut, H. Roche, Y. Plusquellec, F. Peyrille, J. DeBiasi, A. Pujol, P. Canal, and G. Houin. Pharmacokinetic modeling of plasma and cerebrospinal fluid methotrexate after high-dose intravenous infusion in children. *J. Pharm. Sci.* **80**: 730–734 (1991).
2. D. Nierenberg, R. Harbaugh, L. Herbert Mauer, T. Reeder, G. Scott, J. Fratkin, and E. Newman. Continuous intratumoral infusion of methotrexate for recurrent glioblastoma: a pilot study. *Neurosurg.* **28**:752–761 (1991).
3. L. Slordal, R. Jaeger, J. Kjaeve, and J. Aarbakke. Pharmacokinetics of 7-hydroxy-methotrexate and methotrexate in the rat. *Pharmacol. Toxicol.* **63**:81–84 (1988).
4. R. K. Jain, J. Wei, and P. M. Gullino. Pharmacokinetics of methotrexate in solid tumors. *J. Pharmacoki. Biopharm.* **7**:181–194 (1979).
5. P. A. Miglioli, V. Businaro, F. Manoni, and T. Berti. Tissue distribution of methotrexate in rats. Comparison between intravenous injection as bolus or drip infusion. *Drugs Exptl. Clin. Res.* **11**:175–279 (1985).
6. E. C. M. de Lange, J. D. de Vries, C. Zurcher, M. Danhof, A. G. de Boer, and D. D. Breimer. The use of intracerebral microdialysis for the determination of pharmacokinetic profiles of anticancer drugs in tumor-bearing rat brain. *Pharm. Res.* **12**:1924–1931 (1995).
7. D. Devineni, A. Klein-Szanto, and J. M. Gallo. In vivo microdialysis to characterize drug transport in brain tumors: analysis of methotrexate uptake in rat glioma-2 (RG-2)-bearing rats. *Cancer Chemother. Pharmacol.* **38**:499–507 (1996).
8. P. Benda, J. Lightbody, G. Sato, L. Levine, and W. Sweet. Differentiated rat glial cell strain in tissue culture. *Science* **161**:370–371 (1968).
9. S. I. Rapoport, W. R. Fredericks, K. Ohno, and K. D. Pettigrew. Quantitative aspectfs of reversible osmotic opening of the blood-brain barrier. *Am. J. Physiol.* **238**:421–431 (1980).
10. A. Le Quellec, S. Dupin, P. Genissel, S. Saivin, B. Marchand, and G. Houin. Microdialysis probes calibration: Gradient and tissue dependent changes in No Net Flux and Reverse Dialysis methods. *J. Pharmacol. Toxicol. Meth.* **33**:11–16 (1995).
11. M. Gibaldi and D. Perrier. *Pharmacokinetics*, Marcel Dekker, New York, 1982.
12. D. R. Groothuis, J. M. Fischer, J. F. Pasternak, R. G. Blasberg, N. A. Vick, and D. D. Bigner. Reagional measurements of the blood-to-tissue transport in experimental RG-2 rat gliomas. *Cancer Res.* **43**:3368–3373 (1983).
13. P. A. Stewart, K. Hayakawa, E. Hayakawa, C. L. Farrell, and R. F. Del Maestro. A quantitative study of blood-brain barrier permeability ultrastructure in anew rat glioma model. *Acta. Neuropathol. (Berl).* **67**:96–102 (1985).
14. J. J. Bernstein, W. J. Goldberg, E. R. Laws, D. Conger, V. Morreale, and L. R. Wood. C6 glioma cell invasion and migration of rat brain after neural homografting: ultrastructure. *Neurosurg.* **26**:622–628 (1990).
15. V. M. Morreale, B. H. Herman, V. Der-Minassian, M. Palkovits, P. Klubes, D. Perry. A. Csiffary, and A. P. Lee. A brain-tumor model utilizing stereotactic implantation of a permanent cannula. *J. Neurosurg.* **78**:959–965 (1993).
16. N. Kobayashi, N. Allen, N. R. Clendenon, and L. W. Ko. An improved rat brain-tumor model. *J. Neurosurg.* **53**:808–815 (1980).
17. K. Yamada, T. Hayakawa, Y. Ushio, N. Arita, A. Kato, and H. Mogami. Regional blood flow and capillary permeability in the ethylnitrosourea-induced rat glioma. *J. Neurosurg.* **55**:922–928 (1981).
18. B. R. Deane and P. L. Lantos. The vasculature of experimental brain tumors. Part 2. A quantitative assessment of morphological abnormalities. *J. Neurol. Sci.* **49**:67–77 (1981).
19. N. A. Vick, J. D. Khandekar, and D. D. Bigner. Chemotherapy of brain tumors: the 'blood-brain barrier' is not a factor. *Arch. Neurol.* **34**:523–526 (1977).
20. R. M. Bremnes, L. Slordal, E. Wist, and J. Aarbakkle. Dose-dependent pharmacokinetics of methotrexate and 7-hydroxymethotrexate in the rat in vivo. *Cancer Res.* **49**:6359–6364 (1989).
21. P. O. Ekstrom, A. Andersen, D. J. Warren, K. E. Giercksky, and L. Slordal. Pharmacokinetics of different doses of methotrexate at steady state by microdialysis in a rat model. *Cancer Chemother. Pharmacol.* **36**:283–289 (1995).
22. E. Scheufler. Evidence for nonlinear pharmacokinetics of methotrexate in the rat. *Pharmacol.* **25**:51–56 (1982).

23. M. Hammarlund-Udenaes, L. K. Paalzow, and E. C. M. de Lange. Drug equilibration across the blood-brain barrier: Pharmacokinetic considerations based on the microdialysis method. *Pharm. Res.* **14**:128–134 (1997).
24. W. R. Shapiro, R. M. Voorhies, E. M. Hiesiger, P. B. Sher, G. A. Basler, and L. E. Lipschutz. Pharmacokinetics of tumor cell exposure to 14C methotrexate after intracarotid administration without and with hyperosmotic opening of the blood-brain and blood-tumor barriers in rat brain tumors: a quantitative autoradiographic study. *Cancer Res.* **48**:694–701 (1988).
25. D. D. Shen and D. L. Azarnoff. Clinical pharmacokinetics of methotrexate. *Clin. Pharmacokinet.* **3**:1–13 (1978).
26. W. Bleyer and D. G. Pollack. Clinical studies on the central nervous system pharmacology of methotrexate. In: H. M. Pinedo (ed.) *Clinical pharmacology of antineoplastic drugs*. North Holland Biomedical Press, Amsterdam, 1978, pp. 115–130.
27. W. E. Evans, W. R. Crom, and J. C. Yalowich. Methotrexate. In W. E. Evans J. J. Schentag, and W. J. Jusko (eds.), *Applied pharmacokinetics: Principles of therapeutic drug monitoring*, 4th ed., Applied therapeutics, Washington, 1986, pp. 1009–1056.
28. J. H. Schornagel and J. G. McVie. The clinical pharmacology of methotrexate. *Cancer Treat. Rev.* **10**:53–75 (1983).